

# Selectivity Effects on *N,N,N'*-Cobalt Catalyzed Ethylene Dimerization/Trimerization Dictated through Choice of Aluminoxane Cocatalyst

Yongfeng Huang,<sup>†,‡</sup> Randi Zhang,<sup>‡,§</sup> Tongling Liang,<sup>‡</sup> Xinquan Hu,<sup>\*,†</sup> Gregory A. Solan,<sup>\*,‡,||</sup> and Wen-Hua Sun<sup>\*,‡,§,||</sup>

<sup>†</sup>College of Chemical Engineering, Zhejiang University of Technology, Hangzhou 310014, China

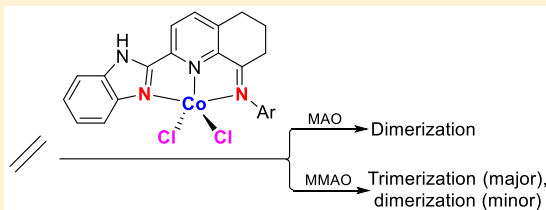
<sup>‡</sup>Key Laboratory of Engineering Plastics and Beijing National Laboratory for Molecular Sciences, Institute of Chemistry, Chinese Academy of Sciences, Beijing 100190, China

<sup>§</sup>CAS Research/Education Center for Excellence in Molecular Sciences and International School, University of Chinese Academy of Sciences, Beijing 100049, China

<sup>||</sup>Department of Chemistry, University of Leicester, University Road, Leicester LE1 7RH, U.K.

## Supporting Information

**ABSTRACT:** The cobalt(II) chloride complexes, [2-(C<sub>7</sub>H<sub>4</sub>N<sub>2</sub>H)-8-(ArN)C<sub>10</sub>H<sub>8</sub>N]CoCl<sub>2</sub> (Ar = 2,6-Me<sub>2</sub>C<sub>6</sub>H<sub>3</sub> **Co1**; 2,6-Et<sub>2</sub>C<sub>6</sub>H<sub>3</sub> **Co2**; 2,6-*i*-Pr<sub>2</sub>C<sub>6</sub>H<sub>3</sub> **Co3**; 2,4,6-Me<sub>3</sub>C<sub>6</sub>H<sub>2</sub> **Co4**; 2,6-Et<sub>2</sub>-4-MeC<sub>6</sub>H<sub>2</sub> **Co5**; 2,4,6-*t*-Bu<sub>3</sub>C<sub>6</sub>H<sub>2</sub> **Co6**), have each been prepared by a one-pot template reaction of 2-benzimidazolyl-5,6,7-trihydroquinolin-8-one with the corresponding aniline in the presence of cobalt dichloride. The molecular structures of the methanol adducts, **Co1**(HOMe) and **Co4**(HOMe), reveal distorted octahedral geometries that self-assemble to form networks based on NH...Cl and OH...Cl intermolecular hydrogen bonding interactions. On activation with methylaluminoxane (MAO), all six cobalt complexes catalyzed ethylene dimerization with a high selectivity for 1-butene. By marked contrast, with modified methylaluminoxane (MMAO), products the result of ethylene dimerization and trimerization were observed with a bias toward the C<sub>6</sub> products (up to 49% 1-hexene). In general, the MMAO-promoted oligomerizations display higher catalytic activities with mesityl-containing **Co4** the stand-out performer [ $7.60 \times 10^5$  g·mol<sup>-1</sup>(Co) h<sup>-1</sup> at 50 °C].



## INTRODUCTION

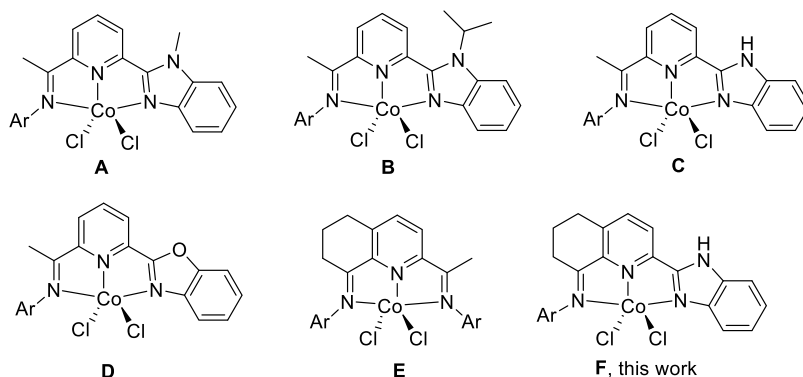
Linear  $\alpha$ -olefins such as 1-butene and 1-hexene are employed, among other things, as comonomers in the manufacture of linear low-density polyethylene (LLDPE). Selective routes to such short chain  $\alpha$ -olefins via the selective dimerization and trimerization of ethylene are known and indeed operated industrially. With regard to dimerization, the AlphaButol process makes use of a homogeneous catalyst based on a combination of titanium tetrabutoxide and triethylaluminum,<sup>1</sup> while trimerization technology largely involves chromium catalysts some of which were originally disclosed by Union Carbide,<sup>2</sup> Chevron-Phillips,<sup>3</sup> and BP.<sup>4</sup> In addition, other first row transition metal catalysts have been investigated for their effectiveness and selectivity in both transformations,<sup>5</sup> though the use of cobalt is less well developed.<sup>6</sup>

Catalysts composed of bis(arylimino)pyridine-iron and cobalt complexes have shown promise for their development in this field as their less sterically demanding derivatives display a preference for ethylene oligomerization over polymerization.<sup>7,8</sup> Indeed, alternative *N,N,N*-cobalt catalysts have emerged that favor the formation of shorter chain oligomers. Among them, cobalt precatalysts based on benzimidazole-substituted pyridylimines have shown a predilection toward

dimers and trimers (Chart 1). Moreover, the nature of the benzimidazole N-R substituent can influence the catalytic performance with alkylated precatalysts of type **A**<sup>8b</sup> or **B**<sup>8c</sup> proving less active than their protio-C counterpart.<sup>8a</sup> On the other hand, substitution of the NH unit in **C** for an O atom in **D**<sup>9</sup> leads to an unusual switch between oligomerization and polymerization as a consequence of the temperature employed.

In recent years, we have found that the introduction of controlled amounts of strain into a bis(imino)pyridine can have an effect on the performance of an ethylene polymerization catalyst. For example, sterically enhanced examples of cyclohexyl-fused **E**<sup>10</sup> on suitable activation function effectively at 60 °C, generating polyethylene waxes, while the corresponding bis(imino)pyridine-cobalt catalyst is much less productive under such high temperature operating conditions.<sup>11</sup> To explore whether a similar structural modification would have beneficial effects on an oligomerization catalyst, we report six examples of benzimidazole-containing **F** in which the steric and electronic properties of the N-aryl group have been systematically varied. An in-depth study is then conducted to

**Received:** December 19, 2018

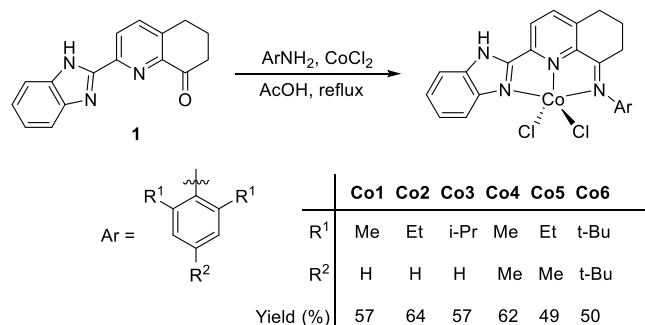
Chart 1. Developments in Unsymmetrical  $N,N,N'$ -Chelating Ligands for Cobalt(II) Chlorides

determine the effects of the precatalyst structure, type and amount of cocatalyst, and temperature on the selectivity of the ethylene oligomerization. Full synthetic and characterization details are additionally presented for the complexes.

## RESULTS AND DISCUSSION

**Synthesis and Characterization of Co1–Co6.** The cobalt(II) chloride complexes,  $[2-(C_7H_4N_2H)-8-(ArN)C_{10}H_8-N]CoCl_2$  ( $Ar = 2,6-Me_2C_6H_3$  **Co1**;  $2,6-Et_2C_6H_3$  **Co2**;  $2,6-i-Pr_2C_6H_3$  **Co3**;  $2,4,6-Me_3C_6H_2$  **Co4**;  $2,6-Et_2-4-MeC_6H_2$  **Co5**;  $2,4,6-t-Bu_3C_6H_2$  **Co6**), were obtained in reasonable yield (49–64%) by templating 2-benzimidazol-6,7-dihydroquinolin-8 (*SH*)-one (**1**) with the corresponding aniline in the presence of cobalt dichloride in acetic acid at reflux (Scheme 1).

Scheme 1. Template Synthetic Route to Co1–Co6



Attempts to prepare the free ligands themselves by an acid catalyzed Schiff base condensation reaction of ketone **1** with the appropriate aniline proved unsuccessful. It is worthy of note that related one-pot template approaches have been applied elsewhere to synthesize similar species.<sup>12</sup> All six cobalt complexes have been characterized by IR spectroscopy as well as by elemental analysis. In addition, the adducts **Co1**(HOMe) and **Co4**(HOMe) have been the subject of single crystal X-ray diffraction studies.

Single crystals of **Co1**(HOMe) and **Co4**(HOMe) suitable for the X-ray determinations were grown by layering diethyl ether onto a solution of the corresponding complex in a methanol/dichloromethane mixture. Perspective views are shown in Figures 1 and 2; selected bond lengths and angles are tabulated in Table 1. The structures of **Co1**(HOMe) and **Co4**(HOMe) are similar and will be discussed together. Each cobalt center is surrounded by two chlorides, one oxygen bound methanol, and three nitrogen atoms belonging to the chelating 2-benzimidazolyl-8-arylimino-5,6,7-trihydroquino-

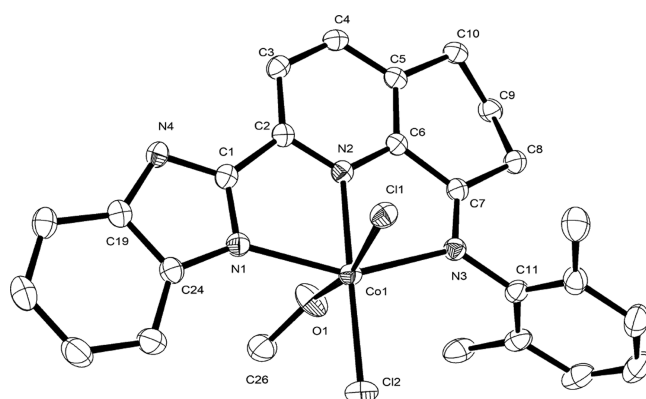


Figure 1. ORTEP representation of **Co1**(HOMe) with the thermal ellipsoids set at the 30% probability level. Hydrogen atoms have been omitted for clarity.

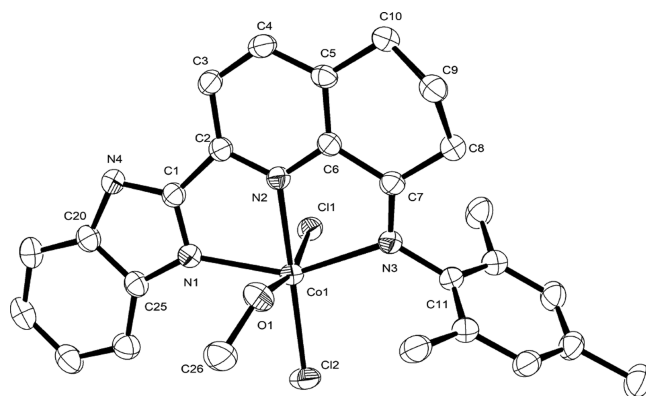


Figure 2. ORTEP representation of **Co4**(HOMe) with the thermal ellipsoids set at the 30% probability level. Hydrogen atoms have been omitted for clarity.

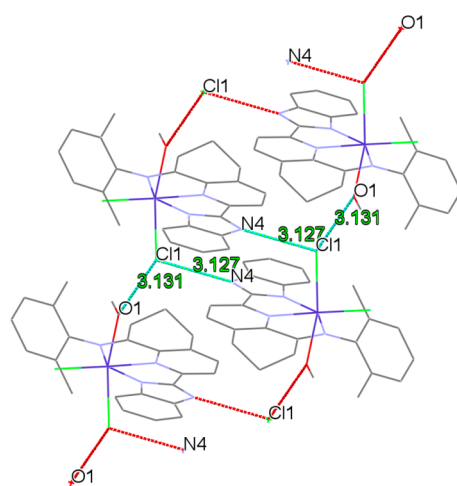
line (aryl =  $2,6-Me_2Ph$  **Co1**;  $2,4,6-Me_3Ph$  **Co4**) to complete a geometry that can be best described as distorted octahedral.<sup>13</sup> The methanol ligand occupies a site *trans* to Cl(1) [ $O(1)-Co(1)-Cl(1)$   $167.57(5)^\circ$  **Co1**,  $166.49(5)^\circ$  **Co4**], while Cl(2) is *trans* to the central nitrogen donor of the *mer*-configured tridentate ligand [ $N(2)-Co(1)-Cl(2)$   $178.49(4)^\circ$  **Co1**,  $177.25(5)^\circ$  **Co4**]; similar  $N,N,N'$ - $CoCl_2$ -(HOMe) adducts have been structurally characterized previously.<sup>8c</sup> Of the three cobalt–nitrogen distances, the one involving the central pyridine is the shortest [ $Co(1)-N(2)$   $2.0895(15)$  Å **Co1**,  $2.0853(17)$  Å **Co4**] while the exterior nitrogen donors show some variation. In particular, the Co–

**Table 1.** Selected Bond Lengths (Å) and Angles (deg) for Co1(HOMe) and Co4(HOMe)

	Co1	Co4
bond lengths		
Co(1)–N(1)	2.1907(15)	2.1842(17)
Co(1)–N(2)	2.0895(15)	2.0853(17)
Co(1)–N(3)	2.2532(15)	2.2471(17)
Co(1)–O(1)	2.2145(16)	2.2682(18)
Co(1)–Cl(1)	2.5600(9)	2.5576(7)
Co(1)–Cl(2)	2.2876(6)	2.2850(6)
N(1)–C(1)	1.323(2)	1.320(3)
N(3)–C(7)	1.285(2)	1.280(3)
N(4)–C(1)	1.355(2)	1.356(3)
bond angles		
N(1)–Co(1)–N(2)	75.40(6)	75.43(6)
N(1)–Co(1)–N(3)	149.50(5)	149.65(6)
N(2)–Co(1)–N(3)	74.31(6)	74.43(6)
N(1)–Co(1)–Cl(2)	105.77(4)	104.69(5)
N(2)–Co(1)–Cl(2)	178.49(4)	177.25(5)
N(3)–Co(1)–Cl(2)	104.46(4)	105.24(5)
N(1)–Co(1)–Cl(1)	87.36(4)	87.86(5)
N(2)–Co(1)–Cl(1)	85.31(5)	86.47(5)
N(3)–Co(1)–Cl(1)	93.67(4)	93.76(5)
Cl(2)–Co(1)–Cl(1)	95.68(3)	96.28(2)
O(1)–Co(1)–Cl(1)	167.57(5)	166.49(5)
O(1)–Co(1)–Cl(2)	95.10(5)	95.64(5)
O(1)–Co(1)–N(1)	83.77(6)	82.99(7)
O(1)–Co(1)–N(2)	84.05(6)	81.63(7)
O(1)–Co(1)–N(3)	89.62(6)	89.20(7)

$N_{\text{benzimidazole}}$  distance is noticeably shorter [Co(1)–N(1) 2.1907(15) Å **Co1**, 2.1842(17) Å **Co4**] than the Co– $N_{\text{imine}}$  distance [Co(1)–N(3) 2.2532(15) Å **Co1**, 2.2471(17) Å **Co4**], reflecting the superior donor properties of the benzimidazole-nitrogen. The Co–Cl bond distances also display some differences with Co(1)–Cl(1) (2.5600(9) Å **Co1**, 2.5576(7) Å **Co4**) notably longer than Co(1)–Cl(2) (2.2876(6) Å **Co1**, 2.2850(6) Å **Co4**), an observation that can be plausibly attributed to the variation in *trans*-donor. Within each 5-membered chelate ring, the bite angles show some modest variation with that involving  $N_{\text{benzimidazole}}$  [N(1)–Co(1)–N(2) 75.41(6)° **Co1**, 75.40(7)° **Co4**] slightly larger than that with  $N_{\text{imine}}$  [N(2)–Co(1)–N(3) 74.31(6)° **Co1**, 74.43(6)° **Co4**], which presumably derives from the constraints of the 5-membered imidazole ring. The imine bond lengths [C(7)–N(3) 1.285(2) Å **Co1**, 1.280(3) Å **Co4**] are typical of this functionality while the *N*-aryl group is inclined almost orthogonally with respect to the imine vector. In each structure, the  $sp^3$ -hybridized C(9) atom belonging to the trihydroquinoline unit is folded away from the plane of the neighboring unsaturated heterocycle with the result that it adopts a confirmation *cis* to the coordinated methanol. Due to the presence of both OH and NH groups within **Co1**(HOMe) and **Co4**(HOMe), an extensive intermolecular hydrogen bonding network is a feature of both structures (Figures 3 and S1). In particular, Cl(1) undergoes both Cl⋯HO and Cl⋯HN interactions with two different neighboring molecules (N(4)⋯Cl(1) 3.127 Å **Co1**; 3.140 Å **Co4**; O(1)⋯Cl(1) 3.131 Å, 3.187 Å) leading to a two-dimensional array within the crystal structure.

The IR spectra of **Co1**–**Co6** reveal imine stretching frequencies in the range 1625–1618  $\text{cm}^{-1}$ , which are

**Figure 3.** NH⋯Cl and OH⋯Cl hydrogen-bonding interactions between neighboring molecules of **Co1**(HOMe).

characteristic of bound imine-nitrogen atoms; no absorption bands corresponding to complexed C=O groups or to free ketone **1** could be detected. In addition, the elemental analysis data confirmed complexes of composition  $\text{LCoCl}_2$ .

**Ethylene Oligomerization.** To explore the role of the cocatalyst, two separate oligomerization studies were performed with each precatalyst using either methylaluminoxane (MAO) or modified methylaluminoxane (MMAO) as the activator. Typically, the oligomerization runs were performed in toluene at 10 atm  $\text{C}_2\text{H}_4$  over 30 min and any selectivity for dimerization, trimerization as well as specific  $\alpha$ -olefins, assessed using gas chromatography (GC); the results of the two studies are gathered in Tables 2 and 3.

**Catalytic Evaluation Using MAO.** To allow an optimization of the conditions, **Co4** was selected as the test precatalyst and the effect of temperature, Al:Co molar ratio, run time, and pressure were all investigated (entries 1–12, Table 2). First, with the Al:Co molar ratio fixed at 1000, the run temperature was increased from 30 to 60 °C and the activity in each case measured after 30 min (entries 1–4, Table 2). The optimum activity of  $1.23 \times 10^5 \text{ g}\cdot\text{mol}^{-1}(\text{Co})\cdot\text{h}^{-1}$  for **Co4**/MAO was observed at 40 °C with a 100% selectivity for ethylene dimerization ( $\text{C}_4$ ) with 1-butene being the major component (91%). Indeed, all runs resulted in solely  $\text{C}_4$  formation with the selectivity for 1-butene decreasing as the temperature was raised.

Second, with the temperature maintained at 40 °C, the Al:Co molar ratio for **Co4**/MAO was increased from 500 to 2000 and the activity determined (entries 2, 5–7, Table 2). On comparison of the four runs, a molar ratio of 1000 resulted in a peak activity of  $1.23 \times 10^5 \text{ g}\cdot\text{mol}^{-1}(\text{Co})\cdot\text{h}^{-1}$ . Once again, only products derived from ethylene dimerization could be detected with the selectivity for 1-butene reducing as the Al:Co molar was raised (e.g.,  $\alpha$ - $\text{C}_4$ : 100% Al:Co = 500; 78% Al:Co = 2000). These decreases in 1-butene content with Al:Co ratio (entries 2, 5–7, Table 2) or reaction temperature can be attributed to the greater thermodynamic stability of internal olefins (e.g., 2-butene).

Third, with the temperature and Al:Co molar ratio fixed at 40 °C and 1000, respectively, the runs using **Co4**/MAO were performed over 5, 15, 45, and 60 min. The highest activity of  $3.17 \times 10^5 \text{ g}\cdot\text{mol}^{-1}(\text{Co})\cdot\text{h}^{-1}$  was observed after 5 min with 1-butene being the only product identifiable. However, this

Table 2. Ethylene Oligomerization Using MAO as Cocatalyst<sup>a</sup>

entry	precatalyst	T [°C]	Al:Co	t [min]	activity <sup>b</sup>	oligomer distribution <sup>c</sup> (%)	
						C <sub>4</sub> /ΣC	α-C <sub>4</sub>
1	Co4	30	1000	30	0.49	100	94.1
2	Co4	40	1000	30	1.23	100	90.8
3	Co4	50	1000	30	0.90	100	85.1
4	Co4	60	1000	30	0.81	100	61.1
5	Co4	40	500	30	0.43	100	100
6	Co4	40	1500	30	0.61	100	84.2
7	Co4	40	2000	30	0.44	100	78.0
8	Co4	40	1000	5	3.17	100	100
9	Co4	40	1000	15	1.52	100	100
10	Co4	40	1000	45	1.06	100	80.5
11	Co4	40	1000	60	0.88	100	71.2
12 <sup>d</sup>	Co4	40	1000	30	0.46	100	91.9
13	Co1	40	1000	30	0.36	100	100
14	Co2	40	1000	30	0.53	100	100
15	Co3	40	1000	30	0.39	100	86.8
16	Co5	40	1000	30	0.77	100	90.6
17	Co6	40	1000	30	0.24	100	94.4

<sup>a</sup>General conditions: 3 μmol of precatalyst, 10 atm C<sub>2</sub>H<sub>4</sub>, 100 mL of toluene. <sup>b</sup>× 10<sup>5</sup> g·mol<sup>-1</sup>(Co)·h<sup>-1</sup>. <sup>c</sup>Determined by GC, and ΣC signifies the total amounts of oligomers. <sup>d</sup>5 atm C<sub>2</sub>H<sub>4</sub>.

Table 3. Ethylene Oligomerization Using MMAO as Cocatalyst<sup>a</sup>

entry	precatalyst	T [°C]	Al:Co	t [min]	activity <sup>b</sup>	oligomer distribution <sup>c</sup> (%)			
						C <sub>4</sub> /ΣC	α-C <sub>4</sub>	C <sub>6</sub> /ΣC	α-C <sub>6</sub>
1	Co4	30	1000	30	4.58	34.0	52.3	66.0	35.0
2	Co4	40	1000	30	4.96	17.3	64.8	82.7	40.3
3	Co4	50	1000	30	7.60	48.5	70.4	51.5	34.6
4	Co4	60	1000	30	4.50	21.4	66.1	78.6	35.1
5	Co4	70	1000	30	3.59	12.9	61.9	87.1	35.7
6	Co4	50	500	30	2.15	30.4	85.9	69.6	35.3
7	Co4	50	1500	30	7.14	15.0	61.6	85.0	35.3
8	Co4	50	2000	30	6.73	6.3	59.1	93.7	35.5
9	Co4	50	1000	5	26.3	16.5	58.0	83.5	35.5
10	Co4	50	1000	15	9.59	11.8	55.7	88.2	35.6
11	Co4	50	1000	45	5.91	8.2	68.7	91.8	35.5
12	Co4	50	1000	60	5.23	7.0	71.6	93.0	36.0
13 <sup>d</sup>	Co4	50	1000	30	6.00	16.0	63.7	84.0	34.9
14 <sup>e</sup>	Co4	50	1000	30	5.12	44.3	75.4	55.7	38.1
15	Co1	50	1000	30	4.76	9.8	57.7	90.2	36.4
16	Co2	50	1000	30	3.55	31.2	62.3	68.8	29.8
17	Co3	50	1000	30	5.28	9.0	47.3	91.0	49.2
18	Co5	50	1000	30	5.31	12.6	56.2	87.4	49.2
19	Co6	50	1000	30	5.64	17.1	62.8	82.9	37.3

<sup>a</sup>General conditions: 3 μmol of precatalyst, 10 atm C<sub>2</sub>H<sub>4</sub>, 100 mL of toluene. <sup>b</sup>10<sup>5</sup> g·mol<sup>-1</sup>(Co)·h<sup>-1</sup>. <sup>c</sup>Determined by GC, and ΣC signifies the total amounts of oligomers. <sup>d</sup>5 atm C<sub>2</sub>H<sub>4</sub>. <sup>e</sup>100 mL of 1,2-xylene as solvent with the conditions otherwise the same as in entry 3.

selectivity for 1-butene gradually decreased over time with only 71.2% selectivity noted after 60 min. With the pressure reduced to 5 bar C<sub>2</sub>H<sub>4</sub>, no loss in selectivity for C<sub>4</sub> products was observed (92% 1-butene) but the activity dropped by more than half (entry 12, Table 2). Overall, these results highlight the importance of reaction temperature, Al:Co ratio, and reaction time on influencing both the selectivity for 1-butene and the catalytic activity.

With the optimized conditions established as temp = 40 °C, Al:Co = 1000, P<sub>C<sub>2</sub>H<sub>4</sub></sub> = 10 atm, the remaining five cobalt precatalysts were similarly screened. In terms of activity (range: 1.23–0.24 × 10<sup>5</sup> g·mol<sup>-1</sup>(Co)·h<sup>-1</sup>), the six precatalysts were found to fall in the order: Co4 > Co5 > Co2 > Co3 ~ Co1 >

Co6. It would appear that both electronic and steric hindrance effects play a combined role on affecting performance with mesityl-containing Co4 the most active and the 2,4,6-tri-*t*-butyl Co6 the least. In particular, *para*-methyl Co4 and Co5 are more active than *para*-H Co1, Co2 and Co3 highlighting the importance of the electron donating *para*-substituent. On the other hand, the most sterically encumbered Co6 likely impedes ethylene coordination, leading to the lowest activity. It is noteworthy that the current systems generally display higher productivities when compared with other *N,N,N*-cobalt oligomerization precatalysts such as A–D (Chart 1).<sup>8,9</sup> Nevertheless, all precatalysts, regardless of *N*-aryl substitution,



gave solely  $C_4$  products with selectivities for 1-butene of greater than 86.7% and indeed 100% for **Co1** and **Co2**.

**Catalytic Evaluation Using MMAO.** As with the MAO study, **Co4** was again used as the test precatalyst to establish the optimized conditions for the runs this time using MMAO as the cocatalyst. The effect of temperature was first explored with the Al:Co ratio set at 1000 (entries 1–5, Table 3). On increasing the temperature from 30 to 70 °C, the highest activity of  $7.60 \times 10^5 \text{ g}\cdot\text{mol}^{-1}(\text{Co})\cdot\text{h}^{-1}$  was observed at 50 °C (entry 3, Table 3), which when compared with the MAO study represents not only a higher operating temperature but also a significantly higher activity (entry 2, Table 2). However, this higher activity is at the expense of poorer selectivity with products now the result of dimerization ( $C_4$ ) and trimerization ( $C_6$ ) evident ( $C_4/\sum C = 48.5\%$ ,  $C_6/\sum C = 51.5\%$ ). Moreover, as the temperature is raised, the bias toward the  $C_6$  products becomes more pronounced (70 °C:  $C_4/\sum C = 12.9\%$ ,  $C_6/\sum C = 87.1\%$ ). With regard to the  $C_6$  products, the selectivity toward 1-hexene remains relatively constant (ca. 35%) between 50 and 70 °C, while, at 40 °C, a greater content of 1-hexene is apparent (up to 40%).

With the temperature of the run retained at 50 °C, the Al:Co molar ratio was increased from 500 to 2000 (entries 3, 6–8). Examination of the data reveals the activity of **Co4**/MMAO reaches its highest value of  $7.60 \times 10^5 \text{ g}\cdot\text{mol}^{-1}(\text{Co})\cdot\text{h}^{-1}$  with an Al:Co molar ratio of 1000 with a gradual drop in the level as the ratio is increased to 2000 (entries 3, 6–8, Table 3). In terms of the oligomer distribution, the preference for  $C_6$  products becomes more evident at higher molar ratios, reaching a maximum of 93.7% at a ratio of 2000. However, the selectivity for 1-hexene remains constant at around 36% for all the Al:Co ratios, highlighting the capacity of these cobalt catalysts to mediate isomerization to give 2-hexene as the major  $C_6$  product.

The effect of time on activity of **Co4**/MMAO shows similar trends to that seen with MAO but with markedly higher activities observed over short run times. Indeed, the highest activity of  $26.3 \times 10^5 \text{ g}\cdot\text{mol}^{-1}(\text{Co})\cdot\text{h}^{-1}$  of the entire study was seen after 5 min, which equates to an 8-fold increase when compared to that seen with MAO after the same time period. As the time elapses, the activity slowly decreases, reaching its lowest value of  $5.23 \times 10^5 \text{ g}\cdot\text{mol}^{-1}(\text{Co})\cdot\text{h}^{-1}$  after 60 min, which is still higher than that seen with MAO after 5 min ( $3.17 \times 10^5 \text{ g}\cdot\text{mol}^{-1}(\text{Co})\cdot\text{h}^{-1}$ , entry 8, Table 3). On the other hand, the bias toward the  $C_6$  products increases with time with the amount of  $C_6$  constituting 93.0% of the mixture after 60 min; the 1-hexene content however remains constant at around 36% over the various reaction times. Lowering the pressure from 10 to 5 atm  $C_2H_4$ , under otherwise identical conditions, saw the activity drop from  $7.60$  to  $6.00 \times 10^5 \text{ g}\cdot\text{mol}^{-1}(\text{Co})\cdot\text{h}^{-1}$  with an increased preference for  $C_6$  products at lower pressure (entries 3 and 13, Table 3). It is worth highlighting that no evidence of octenes could be detected in the GC. Indeed, we ran the oligomerizations in two different aromatic solvents, namely, toluene and 1,2-xylene, to check for any solvent overlap (entry 3, Table 3 vs entry 14, Table 3). In both of these runs, no peaks corresponding to octenes could be observed. Notably, a slightly lower activity was observed in xylene when compared to toluene, but the product distribution was nevertheless similar with hexenes being the major component (more details show in Figures S2 and S3).

Using the optimal conditions established for **Co4**/MMAO (temp = 50 °C, Al:Co = 1000,  $P_{C_2H_4}$  = 10 atm), **Co1**–**Co3** and

**Co6** were additionally screened (entries 3, 15–19, Table 3). Inspection of the tabulated data reveals activities in the range  $7.60$ – $4.76 \times 10^5 \text{ g}\cdot\text{mol}^{-1}(\text{Co})\cdot\text{h}^{-1}$ , with their relative values falling in the order: **Co4** > **Co6** > **Co2** > **Co5** > **Co3** > **Co1**. When compared with the results obtained with MAO, these MMAO-promoted systems not only are more active but also reveal some variations in relative performance with the most sterically hindered system **Co6** now notably toward the top of the order rather than the bottom. Nevertheless, all precatalysts form predominantly products the result of ethylene trimerization rather than dimerization. In terms of the 1-hexene selectivity, some variation is observed between precatalysts with **Co3** and **Co5** affording 49%  $\alpha$ - $C_6$  selectivity while **Co2** only 30%. Compared with previously reported  $N,N,N$ -cobalt oligomerization catalysts (e.g., **A–D**, Chart 1), much higher overall catalytic activity is again a feature of the current systems. Moreover, unlike that observed with **A–D**, ethylene trimerization products have emerged as a major component of the oligomerization distribution. When compared with chromium-based catalysts bearing similar benzimidazole-containing multidentate ligands, the Co/MMAO-type catalysts described in this work show higher selectivity toward trimerization of ethylene and no evidence of polymeric fractions, a byproduct that was a feature of these previous studies.<sup>14</sup> On the other hand, when compared to the well-documented diphosphinoamine(PNP)-type chromium catalysts, the selectivity of the current catalysts for 1-hexene is noticeably less.<sup>15</sup>

In this investigation, the  $C_4/C_6$  composition of short chain alkenes can be influenced by the alkylaluminum activator employed. With MAO, ethylene dimerization was achieved, while, with MMAO, both dimers and trimers were observed. It would appear that the rapid  $\beta$ -H elimination step that occurs under the activation with MAO is influenced by the structural features of the aluminoxane employed. With MMAO, it would seem plausible that the steric properties of the isobutyl groups belonging to this cocatalyst are somehow subtly affecting the active site, leading to competitive ethylene trimerization.

## CONCLUSIONS

Six examples of 2-benzimidazolyl-8-arylimino-5,6,7-trihydroquinoline-cobalt(II) chloride complexes (**Co1**–**Co6**) have been successfully synthesized and fully characterized including in two cases by single crystal X-ray diffraction. On activation with either MAO or MMAO, the current systems exhibited higher catalytic activities for ethylene oligomerization when compared with previously reported  $N,N,N$ -cobalt precatalysts such as **A–D** (Chart 1).<sup>8,9</sup> With MAO as cocatalyst, all the complexes were effective (activities up to  $1.23 \times 10^5 \text{ g}\cdot\text{mol}^{-1}(\text{Co})\cdot\text{h}^{-1}$  for **Co4**) for selective ethylene dimerization ( $C_4$ ) in which 1-butene accounted for the major isomer. By stark contrast, with MMAO as cocatalyst, products the result of ethylene dimerization ( $C_4$ ) and trimerization ( $C_6$ ) were obtained with the  $C_6$  hydrocarbon constituting the major fraction with selectivities for 1-hexene up to 49% (with **Co3** and **Co5**). Moreover, these MMAO-promoted oligomerizations displayed a relatively higher activity (up to  $7.60 \times 10^5 \text{ g}\cdot\text{mol}^{-1}(\text{Co})\cdot\text{h}^{-1}$  for **Co4**) despite the loss of selectivity for dimerization. It is unclear as to the origin of these variations in the  $C_4/C_6$  product distribution that derive from the type of aluminoxane employed and hence will be the subject of further investigations.

## EXPERIMENTAL SECTION

**General Considerations.** All manipulations of air- and/or moisture-sensitive operations were undertaken in a nitrogen atmosphere using standard Schlenk techniques. Toluene was refluxed over sodium and distilled under nitrogen immediately prior to use. Methylaluminoxane (MAO, 1.46 M solution in toluene) and modified methylaluminoxane (MMAO, 1.93 M in *n*-heptane) were purchased from Akzo Nobel Corp. High-purity ethylene was purchased from Beijing Yanshan Petrochemical Co. and used as received. Other reagents were purchased from Aldrich, Acros, or local suppliers. NMR spectra were recorded on a Bruker DMX 400 MHz instrument at ambient temperature using TMS as an internal standard. IR spectra were recorded on a PerkinElmer System 2000 FT-IR spectrometer. GC analyses were performed with a Varian CP-3800 gas chromatograph (Beijing, China) equipped with a flame ionization detector and a 30 m (0.2 mm i.d., 0.25 mm film thickness) CP-Sil 5 CB column. The compound 2-(1*H*-benzimidazol-2-yl)-6,7-dihydroquinolin-8(5*H*)-one (**1**) was prepared as described in the literature.<sup>16</sup>

**Synthesis of [2-(C<sub>7</sub>H<sub>4</sub>N<sub>2</sub>H)-8-(ArN)C<sub>10</sub>H<sub>8</sub>N]CoCl<sub>2</sub>.** Ar = 2,6-Me<sub>2</sub>C<sub>6</sub>H<sub>3</sub> (**Co1**). A suspension of **1** (0.158 g, 0.60 mmol), 2,6-dimethylaniline (0.087 g, 0.72 mmol), and cobalt dichloride (0.074 g, 0.57 mmol) in glacial acetic acid (10 mL) was stirred at reflux for 6 h, affording a brown precipitate. On cooling to room temperature, the precipitate was collected by filtration, washed with diethyl ether (3 × 20 mL) and then dried under reduced pressure, yielding **Co1** as a brown solid (0.160 g, 57%). FT-IR (KBr, cm<sup>-1</sup>): 3031 (w), 2968 (w), 1625 (ν<sub>C=N</sub>, m), 1591 (m), 1488 (w), 1462 (s), 1434 (w), 1423 (w), 1407 (w), 1377 (w), 1352 (w), 1318 (m), 1295 (m), 1263 (m), 1230 (m), 1198 (m), 1106 (m), 1069 (m), 1036 (m), 984 (m), 926 (m), 867 (m), 834 (m), 773 (s), 745 (s), 696 (m), 665 (m). Anal. Calcd for C<sub>24</sub>H<sub>22</sub>Cl<sub>2</sub>CoN<sub>4</sub>: C, 58.08, H, 4.47, N, 11.29. Found: C, 58.46, H, 4.29, N, 10.98%.

Ar = 2,6-Et<sub>2</sub>C<sub>6</sub>H<sub>3</sub> (**Co2**). Using a similar procedure and molar ratios as that described for **Co1**, **Co2** was obtained as a brown powder (0.190 g, 64%). FT-IR (KBr, cm<sup>-1</sup>): 3142 (w), 3114 (w), 3064 (w), 2958 (m), 2930 (m), 2872 (m), 1624 (ν<sub>C=N</sub>, m), 1590 (s), 1453 (s), 1405 (m), 1374 (m), 1323 (m), 1298 (m), 1261 (m), 1240 (m), 1223 (m), 1186 (m), 1145 (m), 1113 (w), 1093 (m), 1057 (m), 1040 (m), 1012 (w), 865 (m), 803 (m), 772 (s), 747 (s), 686 (m), 660 (m). Anal. Calcd for C<sub>26</sub>H<sub>26</sub>Cl<sub>2</sub>CoN<sub>4</sub>: C, 59.56, H, 5.00, N, 10.68. Found: C, 59.87, H, 4.79, N, 10.36%.

Ar = 2,6-*i*-Pr<sub>2</sub>C<sub>6</sub>H<sub>3</sub> (**Co3**). Using a similar procedure and molar ratios as that described for **Co1**, **Co3** was obtained as a brown powder (0.180 g, 57%). FT-IR (KBr, cm<sup>-1</sup>): 3099 (w), 3068 (w), 2962 (s), 2928 (m), 2867 (m), 1618 (ν<sub>C=N</sub>, m), 1590 (m), 1513 (w), 1462 (m), 1442 (m), 1410 (w), 1383 (m), 1359 (m), 1324 (m), 1300 (m), 1271 (m), 1252 (w), 1219 (m), 1184 (m), 1116 (m), 1047 (m), 929 (m), 838 (m), 801.0 (m), 774 (s), 747 (s), 698 (m), 665 (m), 654 (w). Anal. Calcd for C<sub>28</sub>H<sub>30</sub>Cl<sub>2</sub>CoN<sub>4</sub>: C, 60.88, H, 5.47, N, 10.14. Found: C, 61.26, H, 5.25, N, 9.89%.

Ar = 2,6-Et<sub>2</sub>-4-MeC<sub>6</sub>H<sub>2</sub> (**Co4**). Using a similar procedure and molar ratios as that described for **Co1**, **Co4** was obtained as a brown powder (0.180 g, 62%). FT-IR (KBr, cm<sup>-1</sup>): 3058 (m), 2988 (w), 2948 (w), 2914 (w), 2863 (w), 1626 (ν<sub>C=N</sub>, m), 1592 (s), 1461 (s), 1410 (w), 1376 (w), 1349 (m), 1319 (m), 1296 (m), 1269 (m), 1234 (m), 1214 (m), 1149 (m), 1037 (m), 858 (s), 834 (m), 765 (s), 747 (s), 709 (m), 666 (w). Anal. Calcd for C<sub>25</sub>H<sub>24</sub>Cl<sub>2</sub>CoN<sub>4</sub>: C, 58.84, H, 4.74, N, 10.98. Found: C, 59.11, H, 4.49, N, 10.71%.

Ar = 2,6-Et<sub>2</sub>-4-MeC<sub>6</sub>H<sub>2</sub> (**Co5**). Using a similar procedure and molar ratios as that described for **Co1**, **Co5** was obtained as a brown powder (0.150 g, 49%). FT-IR (KBr, cm<sup>-1</sup>): 3142 (w), 2959 (m), 2928 (m), 2871 (m), 1627 (ν<sub>C=N</sub>, m), 1590 (s), 1460 (s), 1435 (w), 1406 (m), 1375 (w), 1326 (m), 1299 (m), 1267 (m), 1210 (m), 1146 (m), 855 (s), 804 (m), 749 (s), 684 (m), 661 (m). Anal. Calcd for C<sub>27</sub>H<sub>28</sub>Cl<sub>2</sub>CoN<sub>4</sub>: C, 60.23, H, 5.24, N, 10.41. Found: C, 60.61, H, 5.01, N, 10.13%.

Ar = 2,4,6-*t*-Bu<sub>3</sub>C<sub>6</sub>H<sub>2</sub> (**Co6**). Using a similar procedure and molar ratios as that described for **Co1**, **Co6** was obtained as a brown powder (0.180 g, 50%). FT-IR (KBr, cm<sup>-1</sup>): 3143 (w), 3112 (w), 3065 (w),

2957 (s), 2904 (w), 2868 (m), 1626 (ν<sub>C=N</sub>, m), 1595 (s), 1489 (w), 1463 (w), 1434 (m), 1393 (m), 1357 (m), 1324 (m), 1297 (m), 1266 (m), 1238 (m), 1208 (s), 1148 (m), 1105 (m), 836 (s), 751 (s), 689 (w), 662 (m). Anal. Calcd for C<sub>34</sub>H<sub>42</sub>Cl<sub>2</sub>CoN<sub>4</sub>: C, 64.15, H, 6.65, N, 8.80. Found: C, 64.48, H, 6.39, N, 8.72%.

**X-ray Crystallographic Studies.** Single crystals of **Co1**(HOME) and **Co4**(HOME) suitable for the X-ray diffraction studies were grown by slow diffusion of *n*-heptane into a solution of the corresponding complex in a mixture of methanol and dichloromethane at room temperature. Data collection for both X-ray determinations was carried out on a Rigaku MM007-HF Saturn 724 + CCD diffractometer with confocal mirror monochromated Mo-*K*α radiation (λ = 0.71073 Å). Cell parameters were obtained by global refinement of the positions of all collected reflections. Intensities were corrected for Lorentz and polarization effects and empirical absorption. The structures were solved by direct methods and refined by full-matrix least-squares on *F*<sup>2</sup>. All hydrogen atoms were placed in calculated positions. Structure solution and refinement were performed by using the SHELXL-97 package.<sup>17</sup> Details of the X-ray structure determination and refinements are provided in Table 4.

**Table 4. Crystal Data and Structure Refinement Details for Co1(HOME) and Co4(HOME)**

	Co1-(HOME)	Co4-(HOME)
formula	C <sub>25</sub> H <sub>26</sub> Cl <sub>2</sub> CoN <sub>4</sub> O	C <sub>26</sub> H <sub>28</sub> Cl <sub>2</sub> CoN <sub>4</sub> O
formula weight	528.33	542.35
<i>T</i> (K)	173	173(2)
wavelength (Å)	0.71073	0.71073
crystal system	monoclinic	monoclinic
space group	<i>P</i> <sub>2</sub> <sub>1</sub> / <i>c</i>	<i>P</i> <sub>2</sub> <sub>1</sub> / <i>c</i>
<i>a</i> (Å)	6.8781(14)	7.0575(2)
<i>b</i> (Å)	20.363(4)	20.0029(6)
<i>c</i> (Å)	16.998(3)	17.2584(5)
α (deg)	90	90
β (deg)	93.68(3)	95.216(3)
γ (deg)	90	90
volume (Å <sup>3</sup> )	2375.7(8)	2426.29(12)
<i>Z</i>	4	4
<i>D</i> <sub>calc</sub> (g cm <sup>-3</sup> )	1.474	1.482
μ (mm <sup>-1</sup> )	0.973	0.955
<i>F</i> (000)	1088	1120
θ range (deg)	4–54.966	4.072–54.958
limiting indices	–6 ≤ <i>h</i> ≤ 8 –26 ≤ <i>k</i> ≤ 24 –20 ≤ <i>l</i> ≤ 22	–9 ≤ <i>h</i> ≤ 8 –24 ≤ <i>k</i> ≤ 25 –22 ≤ <i>l</i> ≤ 22
no. of rflns collected	15414	16612
no. unique rflns [ <i>R</i> (int)]	5416 (0.0254)	5556 (0.0414)
data/restraints/parameters	5416/0/305	5556/0/315
goodness of fit on <i>F</i> <sup>2</sup>	0.607	1.026
final <i>R</i> indices [ <i>I</i> > 2σ( <i>I</i> )]	<i>R</i> <sub>1</sub> = 0.0322 <i>wR</i> <sub>2</sub> = 0.0729	<i>R</i> <sub>1</sub> = 0.0465 <i>wR</i> <sub>2</sub> = 0.1202
<i>R</i> indices (all data)	<i>R</i> <sub>1</sub> = 0.0358 <i>wR</i> <sub>2</sub> = 0.0766	<i>R</i> <sub>1</sub> = 0.0535 <i>wR</i> <sub>2</sub> = 0.1272
largest diff peak and hole (e Å <sup>-3</sup> )	0.34 and –0.24	and –0.30

**Oligomerization of Ethylene. General Procedure.** The ethylene oligomerizations were carried out in a 250 mL stainless steel autoclave equipped with an ethylene pressure control system, a mechanical stirrer, and a temperature controller. The autoclave was evacuated and refilled with ethylene three times. Toluene (50 mL), the desired amount of cocatalyst (MAO or MMAO), and a solution of the precatalyst (**Co1**–**Co6**, 3 μmol) in toluene (50 mL) were successively added by syringe under an ethylene atmosphere, taking the total volume of solvent to 100 mL. When the desired reaction temperature was reached, the stirring was commenced and the ethylene pressure

increased to 10 atm and maintained at this level by a constant feed of ethylene. After 30 min, the reaction was stopped by cooling the reactor in an ice bath and the excess pressure then slowly released. A small amount of this cooled reaction solution was collected (ca. 1 mL) and 5% aqueous hydrogen chloride added to terminate the reaction. A sample of this mixture (0.02  $\mu\text{L}$ ) was then immediately injected into the GC instrument to determine the distribution of oligomers obtained. The mass of  $\text{C}_4$  and  $\text{C}_6$  was calculated based on the ratio of the corresponding peaks to the toluene peak in the gas chromatogram. Since the volume of the toluene ( $n$ ) is fixed, the amount of butenes A ( $n_1$ ) and hexenes B ( $n_2$ ) can be determined (see Tables S1 and S2). Prior to the catalytic evaluations, the retention times for 1-alkenes (1-butene and 1-hexene) and internal alkenes (2-butene, 2-hexene, and 3-hexene) were established. The catalytic activity was based on the mass of all oligomers fractions obtained.

## ■ ASSOCIATED CONTENT

### ● Supporting Information

The Supporting Information is available free of charge on the ACS Publications website at DOI: 10.1021/acs.organomet.8b00924.

The approach to determining the catalytic activity and relative percentage of the products (Tables S1 and S2), the hydrogen-bonding interactions in the crystal structure (Figure S1), and the gas chromatograms (Figures S2–S36) (PDF)

### Accession Codes

CCDC 1871156 and 1871157 contain the supplementary crystallographic data for this paper. These data can be obtained free of charge via [www.ccdc.cam.ac.uk/data\\_request/cif](http://www.ccdc.cam.ac.uk/data_request/cif), or by emailing [data\\_request@ccdc.cam.ac.uk](mailto:data_request@ccdc.cam.ac.uk), or by contacting The Cambridge Crystallographic Data Centre, 12 Union Road, Cambridge CB2 1EZ, UK; fax: +44 1223 336033.

## ■ AUTHOR INFORMATION

### Corresponding Authors

\*E-mail: [xinquan@zjut.edu.cn](mailto:xinquan@zjut.edu.cn) (X.H.).

\*E-mail: [whsun@iccas.ac.cn](mailto:whsun@iccas.ac.cn). Tel: +86-10-62557955. Fax: +86-10-62618239 (W.-H.S.).

\*E-mail: [gas8@leicester.ac.uk](mailto:gas8@leicester.ac.uk). Tel: +44-116-2522096 (G.A.S.).

### ORCID

Wen-Hua Sun: 0000-0002-6614-9284

### Notes

The authors declare no competing financial interest.

## ■ ACKNOWLEDGMENTS

This work was supported by the National Natural Science Foundation of China (No. 21871275). G.A.S. thanks the Chinese Academy of Sciences for a President's International Fellowship for Visiting Scientists.

## ■ REFERENCES

- (1) (a) McGuinness, D. S. Olefin Oligomerization via Metallacycles: Dimerization, Trimerization, Tetramerization, and Beyond. *Chem. Rev.* **2011**, *111*, 2321–2341. (b) Forestière, A.; Olivier-Bourbigou, H.; Saussine, L. Oligomerization of Monoolefins by Homogeneous Catalysts. *Oil Gas Sci. Technol.* **2009**, *64*, 649–667. (c) Metzger, E. D.; Brozek, C. K.; Comito, R. J.; Dincă, M. Selective Dimerization of Ethylene to 1-Butene with a Porous Catalyst. *ACS Cent. Sci.* **2016**, *2*, 148–153.
- (2) (a) Carter, A.; Cohen, S. A.; Cooley, N. A.; Murphy, A.; Scutt, J.; Wass, D. F. High activity ethylene trimerisation catalysts based on diphosphine ligands. *Chem. Commun.* **2002**, *8*, 858–859. (b) Wass, D. F. Olefin trimerisation using a catalyst comprising a source of chromium, molybdenum or tungsten and a ligand containing at least one phosphorous, arsenic or antimony atom bound to at least one (hetero)hydrocarbyl group. U.S. Patent US6800702B2, 2002.
- (3) (a) Dohring, A.; Jensen, V. R.; Jolly, P. W.; Thiel, W.; Weber, J. C. Phosphinoalkyl-Substituted Cyclopentadienyl Chromium Catalysts for the Oligomerization of Ethylene. In *Organometallic Catalysts and Olefin Polymerization*; Springer: Berlin, 2001; pp 127–136. (b) Gibson, V. C.; Redshaw, C.; Solan, G. A. Bis(imino)pyridines: Surprisingly Reactive Ligands and a Gateway to New Families of Catalysts. *Chem. Rev.* **2007**, *107*, 1745–1776. (c) Wang, Z.; Solan, G. A.; Zhang, W.-J.; Sun, W.-H. Carbocyclic-fused *N,N,N*-pincer ligands as ring-strain adjustable supports for iron and cobalt catalysts in ethylene oligo-/polymerization. *Coord. Chem. Rev.* **2018**, *363*, 92–108.
- (4) (a) Broene, R. D.; Brookhart, M.; Lamanna, W. M.; Volpe, A. F., Jr. Cobalt-Catalyzed Dimerization of  $\alpha$ -Olefins to Give Linear  $\alpha$ -Olefin Products. *J. Am. Chem. Soc.* **2005**, *127*, 17194–17195. (b) Thiele, D.; de Souza, R. F. Oligomerization of Ethylene Catalyzed by Iron and Cobalt in Organoaluminate Dialkylimidazolium Ionic Liquids. *Catal. Lett.* **2010**, *138*, 50–55. (c) Zhang, N.; Wang, J.; Huo, H.; Chen, L.; Shi, W.; Li, C.; Wang, J. Iron, cobalt and nickel complexes bearing hyperbranched iminopyridyl ligands: Synthesis, characterization and evaluation as ethylene oligomerization catalysts. *Inorg. Chim. Acta* **2018**, *469*, 209–216. (d) Xu, Z.; Chada, J. P.; Xu, L.; Zhao, D.; Rosenfeld, D. C.; Rogers, J. L.; Hermans, I.; Mavrikakis, M.; Huber, G. W. Ethylene Dimerization and Oligomerization to 1-Butene and Higher Olefins with Chromium-Promoted Cobalt on Carbon Catalyst. *ACS Catal.* **2018**, *8*, 2488–2497. (e) Caovilla, M.; Thiele, D.; de Souza, R. F.; Gregório, J. R.; Bernardo-Gusmão, K. Cobalt- $\beta$ -diimine complexes for ethylene oligomerization. *Catal. Commun.* **2017**, *101*, 85–88. (f) Li, C.; Wang, F.; Lin, Z.; Zhang, N.; Wang, J. Cobalt complexes based on hyperbranched salicylaldimine ligands as catalyst precursors for ethylene oligomerization. *Appl. Organomet. Chem.* **2017**, *31*, No. e3756. (g) Haghighi, M.; Tadjarodi, A.; Bahri-Laleh, N.; Haghighi, M. N. Cobalt complexes based on 2-(1*H*-benzimidazol-2-yl)-phenol derivatives: Preparation, spectral studies, DFT calculations and catalytic behavior toward ethylene oligomerization. *J. Coord. Chem.* **2017**, *70*, 1800–1814.
- (5) (a) Britovsek, G. J. P.; Gibson, V. C.; McTavish, S. J.; Solan, G. A.; White, A. J. P.; Williams, D. J.; Britovsek, G. J. P.; Kimberley, B. S.; Maddox, P. J. Novel olefin polymerization catalysts based on iron and cobalt. *Chem. Commun.* **1998**, 849–850. (b) Britovsek, G. J. P.; Mastroianni, S.; Solan, G. A. S.; Baugh, P. D.; Redshaw, C.; Gibson, V. C.; White, A. J. P.; Williams, D. J. M.; Elsegood, R. J. Oligomerisation of Ethylene by Bis(imino)pyridyliron and -cobalt complexes. *Chem. - Eur. J.* **2000**, *6*, 2221–2231. (c) Small, B. L.; Brookhart, M. Iron-Based Catalysts with Exceptionally High Activities and Selectivities for Oligomerization of Ethylene to Linear  $\alpha$ -Olefins. *J. Am. Chem. Soc.* **1998**, *120*, 7143–7144.
- (6) (a) Small, B. L.; Rios, R.; Fernandez, E. R.; Carney, M. J. Oligomerization of Ethylene Using New Iron Catalysts Bearing Pendant Donor Modified  $\alpha$ -Diimine Ligands. *Organometallics* **2007**, *26*, 1744–1749. (b) Bianchini, C.; Mantovani, G.; Meli, A.; Migliacci, F.; Zanolini, F.; Laschi, F.; Sommazzi, A. Oligomerisation of Ethylene to Linear  $\alpha$ -Olefins by new  $\text{C}_6$ - and  $\text{C}_1$ -Symmetric [2,6-Bis(imino)-pyridyl]iron and -cobalt Dichloride Complexes. *Eur. J. Inorg. Chem.* **2003**, *2003*, 1620–1631. (c) Small, B. L. Tridentate Cobalt Catalysts for Linear Dimerization and Isomerization of  $\alpha$ -Olefins. *Organometallics* **2003**, *22*, 3178–3183. (d) Bianchini, C.; Gatteschi, D.; Giambastiani, G.; Guerrero Rios, I.; Ienco, A.; Laschi, F.; Mealli, C.; Meli, A.; Sorace, L.; Toti, A.; Vizza, F. Electronic Influence of the Thienyl Sulfur Atom on the Oligomerization of Ethylene by Cobalt(II) 6-(Thienyl)-2-(imino)pyridine Catalysts. *Organometallics* **2007**, *26*, 726–739. (e) Bianchini, C.; Giambastiani, G.; Guerrero Rios, I.; Meli, A.; Oberhauser, W.; Sorace, L.; Toti, A. Synthesis of a New Polydentate Ligand Obtained by Coupling 2,6-Bis(imino)-pyridine and (Imino)pyridine Moieties and Its Use in Ethylene Oligomerization in Conjunction with Iron(II) and Cobalt(II) Bishalides. *Organometallics* **2007**, *26*, 5066–5078. (f) Wallenhorst, C.;



- Kehr, G.; Luftmann, H.; Fröhlich, R.; Erker, G. Bis(iminoethyl)-pyridine Systems with a Pendant Alkenyl Group. Part A: Cobalt and Iron Complexes and Their Catalytic Behavior. *Organometallics* **2008**, *27*, 6547–6556. (g) Bianchini, C.; Giambastiani, G.; Guerrero Rios, I.; Mantovani, G.; Meli, A.; Segarra, A. M. Ethylene oligomerization, homopolymerization and copolymerization by iron and cobalt catalysts with 2,6-(bis-organylimino)pyridyl ligands. *Coord. Chem. Rev.* **2006**, *250*, 1391–1418. (h) Zhang, W.; Zhang, W.; Sun, W.-H. The Progress of Late Transition Metal Complexes for Ethylene Oligomerization and Polymerization. *Prog. Chem.* **2005**, *17*, 310–319. (i) Sun, W.-H.; Zhang, S.; Zuo, W.-W. Our variations on iron and cobalt catalysts toward ethylene oligomerization and polymerization. *C. R. Chim.* **2008**, *11*, 307–316. (j) Wang, L.-Y.; Sun, W.-H.; Han, L.-Q.; Yang, H.-J.; Hu, Y.-L.; Jin, X.-L. Late transition metal complexes bearing 2,9-bis(imino)-1,10phenanthroline ligands: synthesis, characterization and their ethylene activity. *J. Organomet. Chem.* **2002**, *658*, 62–70.
- (7) (a) Yu, J.; Huang, W.; Wang, L.; Redshaw, C.; Sun, W.-H. 2-[1-(2,6-Dibenzhydryl-4-methylphenylimino)ethyl]-6-[1-(arylimino)-ethyl]pyridylcobalt(II) dichlorides: Synthesis, characterization and ethylene polymerization behavior. *Dalton Trans.* **2011**, *40*, 10209–10214. (b) Yu, Y.; Liu, H.; Zhang, W.; Hao, X.; Sun, W.-H. Access to highly active and thermally stable iron precatalysts using bulky 2-[1-(2,6-dibenzhydryl-4-methylphenylimino)ethyl]-6-[1-(arylimino)-ethyl]pyridine ligands. *Chem. Commun.* **2011**, *47*, 3257–3259.
- (8) (a) Sun, W.-H.; Hao, P.; Zhang, Z.; Shi, Q.; Zuo, W.; Tang, X.; Lu, X. Iron(II) and Cobalt(II) 2-(Benzimidazolyl)-6-[1-(arylimino)-ethyl]pyridyl Complexes as Catalysts for Ethylene Oligomerization and Polymerization. *Organometallics* **2007**, *26*, 2720–2734. (b) Chen, Y.-J.; Hao, P.; Zuo, W.-W.; Gao, K.; Sun, W.-H. 2-(1-Isopropyl-2-benzimidazolyl)-6-(1-aryliminoethyl)pyridyl transition metal (Fe, Co, and Ni) dichlorides: Syntheses, characterizations and their catalytic behaviors toward ethylene reactivity. *J. Organomet. Chem.* **2008**, *693*, 1829–1840. (c) Xiao, L.-W.; Gao, R.; Zhang, M.; Li, Y.; Cao, X.-P.; Sun, W.-H. 2-(1H-2-Benzimidazolyl)-6-(1-(arylimino)ethyl)pyridyl Iron(II) and Cobalt(II) Dichlorides: Syntheses, Characterizations, and Catalytic Behaviors toward Ethylene Reactivity. *Organometallics* **2009**, *28*, 2225–2233.
- (9) Gao, R.; Wang, K.-F.; Li, Y.; Wang, F.-S.; Sun, W.-H.; Redshaw, C.; Bochmann, M. 2-Benzoxazolyl-6-(1-(arylimino)ethyl)-pyridylcobalt(II)chlorides: A temperature switch catalyst in oligomerization and polymerization of ethylene. *J. Mol. Catal. A: Chem.* **2009**, *309*, 166–171.
- (10) Sun, W.-H.; Kong, S.; Chai, W.; Shiono, T.; Redshaw, C.; Hu, X.; Guo, C.; Hao, X. 2-(1-(Arylimino)ethyl)-8-arylimino-5,6,7-trihydroquinolylcobalt dichloride: Synthesis and polyethylene wax formation. *Appl. Catal., A* **2012**, *447*–*448*, 67–73.
- (11) (a) Flisak, Z.; Sun, W.-H. Progression of Diiminopyridines: from Single Application to Catalytic Versatility. *ACS Catal.* **2015**, *5*, 4713–4724. (b) Ma, J.; Feng, C.; Wang, S.; Zhao, K.-Q.; Sun, W.-H.; Redshaw, C.; Solan, G. A. Bi- and tri-dentate Imino-Based Iron and Cobalt Pre-catalysts for Ethylene Oligo-/Polymerization. *Inorg. Chem. Front.* **2014**, *1*, 14–34. (c) Gibson, V. C.; Solan, G. A. Iron-Based and Cobalt-Based Olefin Polymerisation Catalysts. *Top. Organomet. Chem.* **2009**, *26*, 107–158. (d) Gibson, V. C.; Solan, G. A. Olefin Oligomerizations and Polymerizations Catalyzed by Iron and Cobalt Complexes Bearing Bis(imino)pyridine Ligands. In *Catalysis without Precious Metals*; Bullock, R. M., Ed.; Wiley-VCH: Weinheim, Germany, 2010; pp 111–141.
- (12) (a) Zhang, M.; Wang, K.-F.; Sun, W.-H. Chromium(III) complexes bearing 2-benzazole-110-phenanthrolines: Synthesis molecular structures and ethylene oligomerization and polymerization. *Dalton Trans* **2009**, 6354–6363. (b) Yin, Y.-Z.; Yue, X.-Y.; Zhong, Q.; Jiang, H.-M.; Bai, R.-P.; Lan, Y.; Zhang, H. Front Cover Picture: A Structure-Based Activity Study of Highly Active Unsymmetrically Substituted NHC Gold(I) Catalysts. *Adv. Synth. Catal.* **2018**, *360*, 1–6.
- (13) (a) Sun, W.-H.; Wang, K.; Wedeking, K.; Zhang, D.; Zhang, S.; Cai, J.; Li, Y. Synthesis, Characterization, and Ethylene Oligomerization of Nickel Complexes Bearing N-((Pyridin-2-yl)methylene)-quinolin-8-amine Derivatives. *Organometallics* **2007**, *26*, 4781–4790. (b) Wang, K.; Wedeking, K.; Zuo, W.; Zhang, D.; Sun, W.-H. Iron(II) and cobalt(II) complexes bearing N-((pyridin-2-yl)methylene)-quinolin-8-amine derivatives: Synthesis and application to ethylene oligomerization. *J. Organomet. Chem.* **2008**, *693*, 1073–1080. (c) Appukkuttan, V. K.; Liu, Y.; Son, B. C.; Ha, C.; Suh, H.; Kim, I. Iron and Cobalt Complexes of 2,3,7,8-Tetrahydroacridine-4,5-(1H,6H)-diimine Sterically Modulated by Substituted Aryl Rings for the Selective Oligomerization to Polymerization of Ethylene. *Organometallics* **2011**, *30*, 2285–2294.
- (14) (a) Xiao, L.; Zhang, M.; Sun, W.-H. Synthesis, characterization and ethylene oligomerization and polymerization of 2-(1H-2-benzimidazolyl)-6-(1-(arylimino)ethyl) pyridylchromium chlorides. *Polyhedron* **2010**, *29*, 142–147. (b) Zhang, W.; Sun, W.-H.; Zhang, S.; Hou, J.; Wedeking, K.; Schultz, S.; Fröhlich, R.; Song, H. Synthesis, Characterization, and Ethylene Oligomerization and Polymerization of [2,6-Bis(2-benzimidazolyl)pyridyl]chromium Chlorides. *Organometallics* **2006**, *25*, 1961–1969. (c) Bariashir, C.; Huang, C.; Solan, G. A.; Sun, W.-H. Recent advances in homogeneous chromium catalyst design for ethylene tri-, tetra-, oligo- and polymerization. *Coord. Chem. Rev.* **2019**, *385*, 208–229.
- (15) Wass, D. F. Chromium-catalysed ethene trimerisation and tetramerisation—breaking the rules in olefin oligomerisation. *Dalton Trans* **2007**, 816–819.
- (16) (a) Wang, Z.; Solan, G. A.; Mahmood, Q.; Liu, Q.-B.; Ma, Y.-P.; Hao, X.; Sun, W.-H. Bis(imino)pyridines Incorporating Doubly Fused Eight-Membered Rings as Conformationally Flexible Supports for Cobalt Ethylene Polymerization Catalysts. *Organometallics* **2018**, *37*, 380–389. (b) Lai, J.-J.; Zhao, W.-Z.; Yang, W.-H.; Redshaw, C.; Liang, T.-L.; Liu, Y.-G.; Sun, W.-H. 2-[1-(2,4-Dibenzhydryl-6-methylphenylimino)ethyl]-6-[1-(arylimino)ethyl]pyridylcobalt(II) dichlorides: Synthesis, characterization and ethylene polymerization behavior. *Polym. Chem.* **2012**, *3*, 787–793. (c) Ba, J.-J.; Du, S.-Z.; Yue, E.; Hu, X.-Q.; Flisak, Z.; Sun, W.-H. Constrained formation of 2-(1-(arylimino)ethyl)-7-arylimino-6,6-dimethylcyclopentapyridines and their cobalt(II) chloride complexes: synthesis, characterization and ethylene polymerization. *RSC Adv.* **2015**, *5*, 32720–32729. (d) Huang, F.; Zhang, W.-J.; Sun, Y.; Hu, X.-Q.; Solan, G. A.; Sun, W.-H. Thermally stable and highly active cobalt precatalysts for vinyl-polyethylenes with narrow polydispersities: integrating fused-ring and imino-carbon protection into ligand design. *New J. Chem.* **2016**, *40*, 8012–8023.
- (17) (a) Sheldrick, G. M. SHELXT – Integrated space-group and crystal-structure determination. *Acta Crystallogr., Sect. A: Found. Adv.* **2015**, *A71*, 3–8. (b) Sheldrick, G. M. Crystal structure refinement with SHELXL. *Acta Crystallogr., Sect. C: Struct. Chem.* **2015**, *C71*, 3–8.